

# Light $1^{-+}$ exotics: Molecular resonances

Ignacio J. General<sup>a,\*</sup>, Ping Wang<sup>a</sup>, Stephen R. Cotanch<sup>a</sup>, Felipe J. Llanes-Estrada<sup>b</sup>

<sup>a</sup> Department of Physics, North Carolina State University, Raleigh, NC 27695-8202, USA

<sup>b</sup> Departamento de Física Teórica I, Universidad Complutense, 28040 Madrid, Spain

Received 11 July 2007; received in revised form 31 July 2007; accepted 8 August 2007

Available online 11 August 2007

Editor: B. Grinstein

## Abstract

Highlights in the search for nonconventional (non- $q\bar{q}$ ) meson states are the  $\pi_1(1400)$  and  $\pi_1(1600)$  exotic candidates. Should they exist, mounting theoretical arguments suggest that they are tetraquark molecular resonances excitable by meson rescattering. We report a new tetraquark calculation within a model field theory approximation to Quantum Chromodynamics in the Coulomb gauge supporting this conjecture. We also strengthen this claim by consistently contrasting results with exotic state predictions for hybrid ( $q\bar{q}g$ ) mesons within the same theoretical framework. Our findings confirm that molecular-like configurations involving two color singlets (a resonance, not a bound state) are clearly favored over hybrid or color-exotic tetraquark meson ( $q\bar{q}q\bar{q}$  atoms) formation. Finally, to assist needed further experimental searches we document a useful off-plane correlator for establishing the structure of these exotic systems along with similar, but anticipated much narrower, states that should exist in the charmonium and bottomonium spectra.

© 2007 Elsevier B.V. All rights reserved.

PACS: 12.39.Mk; 12.39.Pn; 12.39.Ki; 12.40.Yx

Keywords: Exotic mesons; Tetraquarks; QCD Coulomb gauge; Effective Hamiltonian

## 1. Introduction

The existence and understanding of exotic (non- $q\bar{q}$  and  $qqq$ ) hadrons is one of the few remaining closures to the standard model. Such states are expected according to Quantum Chromodynamics (QCD) and are of intense experimental interest. In the light quark sector, there are two published isovector candidates at 1.3–1.4 and 1.6 GeV,  $\pi_1(1400)$  and  $\pi_1(1600)$ , each having  $J^{PC} = 1^{-+}$  [1,2]. The signature is observed as a p-wave resonance in the  $\eta\pi^0$  system and it therefore has odd parity  $P$  but even charge conjugation  $C$  yielding the quantum numbers  $J^{PC} = 1^{-+}$ . Since a  $q\bar{q}$  state with orbital  $L$  and spin  $S$  coupled to  $J = 1$  must have  $P = (-1)^{L+1}$  and  $C = (-1)^{L+S}$ , this state is clearly exotic. More recent partial wave analyses for these states have produced contradictory results with Ref. [3] finding no evidence for either  $\pi_1$  while Ref. [4] reconfirms the  $\pi_1(1400)$ . For further discussion consult Ref. [5].

Assuming these states exist, the theoretical situation is even more controversial. The debate concerning their structure is among four possible scenarios: (1) a hybrid ( $q\bar{q}g$ ) meson; (2) a tetraquark atom ( $q\bar{q}q\bar{q}$  involving intermediate color states that are not singlets); (3) a tetraquark molecular bound state of two conventional mesons; (4) a tetraquark molecular resonance ( $q\bar{q}q\bar{q}$  involving two intermediate color states that are singlets but not observed mesons). All four scenarios can produce  $J^{PC} = 1^{-+}$  states but the first two are more exotic since the tetraquark molecule is color equivalent to a conventional meson-meson two-body state (see Fig. 1).

\* Corresponding author.

E-mail address: [ijgeneral@gmail.com](mailto:ijgeneral@gmail.com) (I.J. General).

<sup>1</sup> Current address: Bayer School of Natural and Environmental Sciences, Duquesne University, Pittsburgh, PA 15282, USA.

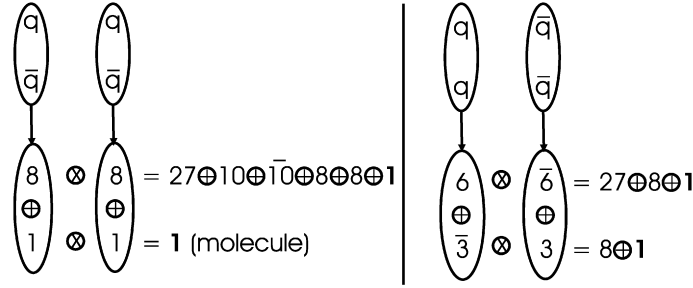


Fig. 1. Four independent tetraquark color schemes. One is a singlet-singlet molecule while the other three are more exotic atoms (octet and two diquark schemes).

Lattice results, now performed with more realistic lower quark masses [6], have focused upon the hybrid scenario but find that hybrid correlators can only produce a state as low as 1.9 to 2.1 GeV. A more recent lattice calculation [7] claims to find two hybrid meson masses below 2 GeV, however their extrapolation, that is quadratic in the pion mass, to these lower values entails uncertainty since decay thresholds open with cusps having unknown coupling strengths. Similarly, the lightest Flux Tube model  $1^{-+}$  predictions [8–10] are also near 2 GeV spanning the region of 1.8 to 2.1 GeV. This is consistent with agreement among other model approaches, based on either the concept of constituent gluons [11] or field-theory calculations (see below) generating mass-gaps [12], that the lightest hybrid mesons with just one constituent gluon should be somewhat heavier than the 1.4, 1.6 GeV experimental candidates. Finally, both well-established spin [13] and flavor [14] selection rules indicate that the above mentioned  $\eta\pi$  signature cannot be due to hybrid meson decay. It appears that the  $\pi_1$  states can not be theoretically explained as hybrids.

In search of other explanations, a potential model lifetime calculation [15] has ruled out a molecular  $\eta(1295)\pi$  or  $\eta(1440)\pi$  bound state. However, it has been shown that meson-rescattering, specifically in the  $\eta\pi$  channel, could produce a resonance with this signature [16,17]. Also, it has been suggested [18] that the 1.6 GeV resonance could be interfering with a background to produce the 1.4 GeV structure.

Summarizing the status of this situation, while the  $\pi_1(1600)$  cannot be firmly precluded as a hybrid meson or exotic tetraquark, the  $\pi_1(1400)$  seems explainable only as a molecular resonance excited by meson rescattering. The purpose of this work is to confirm the latter by a new theoretical analysis which also predicts that the  $\pi_1(1600)$  is not a color exotic system. Our formalism, referred to as the Coulomb Gauge Model (CGM), has been successfully established in both the quark [19–21] and gluon [22] sectors and is based upon the exact QCD Hamiltonian in the Coulomb gauge [23] given by

$$H_{\text{QCD}} = H_q + H_g + H_{qg} + H_C, \quad (1)$$

$$H_q = \int d\mathbf{x} \Psi^\dagger(\mathbf{x}) [-i\boldsymbol{\alpha} \cdot \nabla + \beta m] \Psi(\mathbf{x}), \quad (2)$$

$$H_g = \frac{1}{2} \int d\mathbf{x} [\mathcal{J}^{-1} \boldsymbol{\Pi}^a(\mathbf{x}) \cdot \mathcal{J} \boldsymbol{\Pi}^a(\mathbf{x}) + \mathbf{B}^a(\mathbf{x}) \cdot \mathbf{B}^a(\mathbf{x})], \quad (3)$$

$$H_{qg} = g \int d\mathbf{x} \mathbf{J}^a(\mathbf{x}) \cdot \mathbf{A}^a(\mathbf{x}), \quad (4)$$

$$H_C = -\frac{g^2}{2} \int d\mathbf{x} d\mathbf{y} \rho^a(\mathbf{x}) \mathcal{J}^{-1} K^{ab}(\mathbf{x}, \mathbf{y}) \mathcal{J} \rho^b(\mathbf{y}). \quad (5)$$

Here  $g$  is the QCD coupling,  $\Psi$  the quark field with current quark mass  $m$ ,  $\mathbf{A}^a$  the gluon fields satisfying the transverse gauge condition,  $\nabla \cdot \mathbf{A}^a = 0$ ,  $a = 1, 2, \dots, 8$ ,  $\boldsymbol{\Pi}^a$  the conjugate fields and  $\mathbf{B}^a$  the non-Abelian magnetic fields,  $\mathbf{B}^a = \nabla \times \mathbf{A}^a + \frac{1}{2} g f^{abc} \mathbf{A}^b \times \mathbf{A}^c$ . The color densities,  $\rho^a(\mathbf{x}) = \Psi^\dagger(\mathbf{x}) T^a \Psi(\mathbf{x}) + f^{abc} \mathbf{A}^b(\mathbf{x}) \cdot \boldsymbol{\Pi}^c(\mathbf{x})$ , and quark color currents,  $\mathbf{J}^a = \Psi^\dagger(\mathbf{x}) \boldsymbol{\alpha} T^a \Psi(\mathbf{x})$ , entail the  $SU_c(3)$  color matrices,  $T^a = \frac{\lambda^a}{2}$ , and structure constants,  $f^{abc}$ . The Faddeev-Popov determinant,  $\mathcal{J} = \det(\mathcal{M})$ , of the matrix  $\mathcal{M} = \nabla \cdot \mathbf{D}$  with covariant derivative  $\mathbf{D}^{ab} = \delta^{ab} \nabla - g f^{abc} \mathbf{A}^c$ , is a measure of the gauge manifold curvature and the kernel in Eq. (5) is given by  $K^{ab}(\mathbf{x}, \mathbf{y}) = \langle \mathbf{x}, a | \mathcal{M}^{-1} \nabla^2 \mathcal{M}^{-1} | \mathbf{y}, b \rangle$ . The Coulomb gauge Hamiltonian is renormalizable, permits resolution of the Gribov problem, preserves rotational invariance, avoids spurious retardation corrections, aids identification of dominant, low energy potentials and does not introduce unphysical degrees of freedom (ghosts) [24]. To make the problem tractable, the Coulomb instantaneous kernel is approximated by its vacuum expectation value, yielding an effective potential field theory,  $H_{\text{QCD}} \rightarrow H_{\text{QCD}}^{\text{eff}}$ ,

$$H_C \rightarrow H_C^{\text{eff}} = -\frac{1}{2} \int d\mathbf{x} d\mathbf{y} \rho^a(\mathbf{x}) \hat{V}(|\mathbf{x} - \mathbf{y}|) \rho^a(\mathbf{y}), \quad (6)$$

with confinement described by a Cornell potential,  $\hat{V}(r) = -\frac{\alpha_s}{r} + \sigma r$ , where the string tension,  $\sigma = 0.135 \text{ GeV}^2$ , and  $\alpha_s = 0.4$  have been independently determined from conventional meson studies [19–21] within the same field theory approach. We also use the lowest order, unit value, for the Faddeev-Popov determinant in the  $H_g$  term and treat the  $H_{qg}$  interaction using perturbation theory. Lattice data confirms the Cornell potential form between static sources [25] and further provides the scale of the gluon mass

gap [26], that is needed to fit a counterterm in the gluon gap equation. The remaining parameters are the reasonably well known current quark masses at some high energy scale where the mass function runs perturbatively. The quark sector Hamiltonian then takes the form of the Cornell coupled-channel model [27]. We note that three-body forces [28,29] are omitted, however based upon successful three-body applications [22] we submit the CGM should capture the dominant features of a multi-parton spectrum.

Before presenting our tetraquark results we highlight our recent hybrid meson calculation [30]. Since the gluon carries a color octet charge, the quark and anti-quark are also in a color octet wavefunction with elements  $T_{ij}^a$  (they repel each other at short distance). In the hybrid rest frame there are two independent three-momenta  $\mathbf{q}_+ = \frac{\mathbf{q} + \bar{\mathbf{q}}}{2}$ ,  $\mathbf{q}_- = \mathbf{q} - \bar{\mathbf{q}}$  and one dependent  $\mathbf{g} = -\mathbf{q} - \bar{\mathbf{q}} = -2\mathbf{q}_+$ . The leading hybrid Fock space wavefunction can therefore be constructed from the respective quark, anti-quark and gluon quasiparticle operators  $B_{\lambda_1 C_1}^\dagger(\mathbf{q})$ ,  $D_{\lambda_2 C_2}^\dagger(\bar{\mathbf{q}})$  and  $\alpha_\mu^{a\dagger}(\mathbf{g})$

$$|\Psi^{JPC}\rangle = \iint \frac{d\mathbf{q}_+}{(2\pi)^3} \frac{d\mathbf{q}_-}{(2\pi)^3} \Phi_{\lambda_1 \lambda_2 \mu}^{JPC}(\mathbf{q}_+, \mathbf{q}_-) T_{C_1 C_2}^a B_{\lambda_1 C_1}^\dagger(\mathbf{q}) D_{\lambda_2 C_2}^\dagger(\bar{\mathbf{q}}) \alpha_\mu^{a\dagger}(\mathbf{g}) |\Omega\rangle. \quad (7)$$

An angular momentum expansion for the lightest  $1^{-+}$  state reveals a required p-wave excitation in one of the two orbital wavefunctions. Consult Ref. [30] for complete details. Significantly, in agreement with earlier findings [12], the predicted hybrid masses are about 2 GeV for the ground state (parity +) quadruplet and 2.2 and 2.4 GeV, respectively, for the first  $1^{-+}$  exotics. The repulsive nature of the short range  $q\bar{q}$  interaction potential kernel and the large gluon mass gap are responsible for these large masses. We also performed a parameter sensitivity and error analysis study and concluded there was no model possibility to lower one of these states near the 1.6 GeV candidate and therefore rule out this, and even more clearly the 1.4 GeV, state as a hybrid.

Returning to our thrust, we report results for  $qq\bar{q}\bar{q}$  spectroscopy (see also a preliminary study [31]). This system was first investigated in the bag model [32] and then more extensively by Ref. [33] with subsequent potential model applications reported by Refs. [34,35]. While these studies have some similarity to our model, we submit our results are more robust since our approach is much more comprehensive, has many QCD elements with no new parameters to be determined and employs a realistic potential kernel extracted from lattice gauge theory. The leading tetraquark Fock space wavefunction is [36,37]

$$|\Psi^{JPC}\rangle = \iiint \frac{d\mathbf{q}_A}{(2\pi)^3} \frac{d\mathbf{q}_B}{(2\pi)^3} \frac{d\mathbf{q}_I}{(2\pi)^3} \Phi_{\lambda_1 \lambda_2 \lambda_3 \lambda_4}^{JPC}(\mathbf{q}_A, \mathbf{q}_B, \mathbf{q}_I) R_{C_3 C_4}^{C_1 C_2} B_{\lambda_1 C_1}^\dagger(\mathbf{q}_1) D_{\lambda_2 C_2}^\dagger(\mathbf{q}_2) B_{\lambda_3 C_3}^\dagger(\mathbf{q}_3) D_{\lambda_4 C_4}^\dagger(\mathbf{q}_4) |\Omega\rangle. \quad (8)$$

In the  $cm$  there are three independent momenta which we take to be  $\mathbf{q}_A = \frac{\mathbf{q}_1 - \mathbf{q}_2}{2}$ ,  $\mathbf{q}_B = \frac{\mathbf{q}_3 - \mathbf{q}_4}{2}$  and  $\mathbf{q}_I = \frac{\mathbf{q}_3 + \mathbf{q}_4}{2} - \frac{\mathbf{q}_1 + \mathbf{q}_2}{2}$  ( $\mathbf{q}_1, \mathbf{q}_3$  for the quarks and  $\mathbf{q}_2, \mathbf{q}_4$  for the anti-quarks). The color matrices  $R_{C_3 C_4}^{C_1 C_2}$  yielding color-singlet wavefunctions follow from the  $SU_c(3)$  algebra depicted in Fig. 1. The radial part of  $\Phi_{\lambda_1 \lambda_2 \lambda_3 \lambda_4}^{JPC}(\mathbf{q}_A, \mathbf{q}_B, \mathbf{q}_I)$  is chosen to be a Gaussian,  $\exp(-\frac{q_A^2}{\alpha_A^2} - \frac{q_B^2}{\alpha_B^2} - \frac{q_I^2}{\alpha_I^2})$ , with variational parameters  $\alpha_A, \alpha_B$  and  $\alpha_I$  for s-wave states and a Gaussian multiplied by  $q_i^2/\alpha_i^2$  ( $i = A, B, I$ ) corresponding to orbital  $L_i = 1$ , when treating p-wave states. Note, as for hybrid mesons, the ground state tetraquark multiplet has positive parity and that constructing  $1^{-+}$  exotics requires one of the three orbitals to be a p-wave. Using the variational principle, the tetraquark mass is then given by

$$M_{JPC} \leq \frac{\langle \Psi^{JPC} | H_{\text{QCD}}^{\text{eff}} | \Psi^{JPC} \rangle}{\langle \Psi^{JPC} | \Psi^{JPC} \rangle} = M_{\text{self}} + M_{q\bar{q}} + M_{\bar{q}q} + M_{q\bar{q}} + M_{\text{annih}}. \quad (9)$$

Contributions to the Hamiltonian expectation value are summarized in Fig. 2 and correspond consecutively to 4 self-energy, 6 scattering, 4 annihilation and 70 exchange terms, each of which can be reduced to 12 dimensional integrals that are evaluated

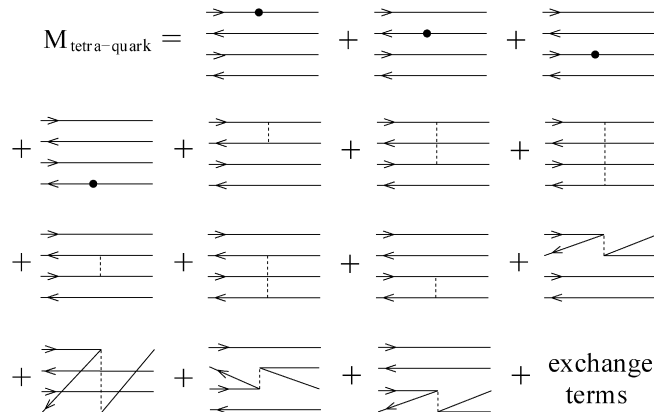


Fig. 2. Equal-time diagrams for  $\langle \Psi^{JPC} | H_{\text{QCD}}^{\text{eff}} | \Psi^{JPC} \rangle$ . Arrows to the right (left) represent quarks (anti-quarks). Vertical lines indicate instantaneous Cornell coupling.

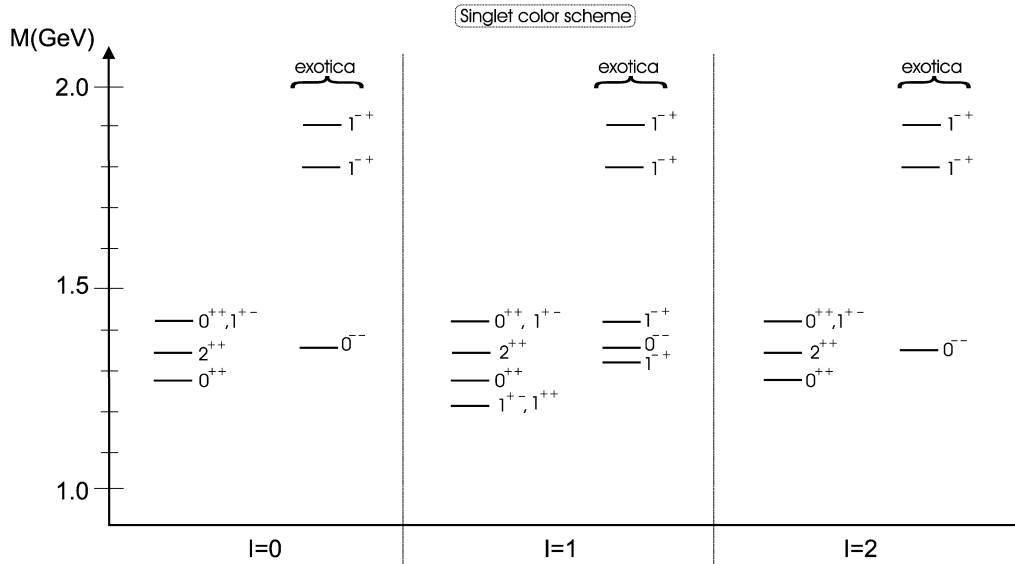


Fig. 3. Low-lying  $I = 0, 1$  and  $2$  spectrum for the singlet (molecule) scheme.

in momentum space. Because of the computationally intensive nature of this analysis, the hyperfine interaction was not included. Complete expressions will be given in another publication, but as an example note the annihilation contribution, not possible in standard quark models, is

$$M_{\text{annih}} = \iiint \frac{d\mathbf{q}_1 d\mathbf{q}_2 d\mathbf{q}_3 d\mathbf{k}}{(2\pi)^{12}} V(\mathbf{q}_1 + \mathbf{q}_2) u_{\lambda'_1}^\dagger(\mathbf{q}_1 + \mathbf{k}) v_{\lambda'_2}(\mathbf{q}_2 - \mathbf{k}) \times v_{\lambda_2}^\dagger(\mathbf{q}_2) u_{\lambda_1}(\mathbf{q}_1) \Phi_{\lambda_1 \lambda_2 \lambda_3 \lambda_4}^{JPC\dagger}(\mathbf{q}_1, \mathbf{q}_2, \mathbf{q}_3) \Phi_{\lambda'_1 \lambda'_2 \lambda_3 \lambda_4}^{JPC}(\mathbf{q}_1 + \mathbf{k}, \mathbf{q}_2 - \mathbf{k}, \mathbf{q}_3), \quad (10)$$

involving Dirac spinors  $u_{\lambda_1}$  and  $v_{\lambda_2}$ . This raises the mass of the isoscalar states relative to the states with higher isospin, which would otherwise typically be heavier due to the exclusion principle applied to equal-flavor quarks.

Performing large-scale Monte Carlo calculations (typically 50 million samples), has conclusively determined that the molecular representation (i.e. singlet–singlet) produces the lightest mass for a given  $J^{PC}$ . This is due to suppression of certain interactions in this color scheme from vanishing color factors for every parton pair which does not occur in the other representations. Also, there are additional, repulsive forces in the more exotic color schemes. Using  $m_u = m_d = 5$  MeV, the predicted tetraquark ground state is the non-exotic vector  $1^{++}$  state in the molecular representation with mass around 1.2 GeV. Fig. 3 depicts the predicted tetraquark spectra for states having conventional and exotic quantum numbers in the singlet color representation. The quark annihilation interactions ( $q\bar{q} \rightarrow g \rightarrow q\bar{q}$ ) in the  $I_{q\bar{q}} = 0$  channel generate isospin splitting contributions, up to several hundred MeV, in the octet (not shown) but not singlet scheme. Isospin splitting is a consequence of a more proper field theory treatment, not present in conventional quark models. The annihilation interaction terms are repulsive, yielding octet states with  $I = 2$  lower than the  $I = 1$  which are lower than the  $I = 0$ . This is intuitively contrary to expectations that  $I = 2$  states are higher based upon the Pauli principle that identical quarks repel. The singlet scheme molecular states are all isospin degenerate and the lightest exotic molecule is an intriguing  $0^{-}$  with mass 1.36 GeV that could be detected in a sophisticated p-wave analysis of an  $\omega\pi$  spectrum. Because of the isospin degeneracy, there will be several molecular tetraquark states with the same  $J^{PC}$  in the 1 to 2 GeV region. Further, these states can be observed in different electric charge channels (different  $I_z$ ) at about the same energy, which is a useful experimental signature.

The lightest  $1^{-}$  are the two  $I = 1$  states at 1.32 and 1.42 GeV, close to the observed  $\pi(1400)$ , suggesting this state has a molecular resonance structure. The computed mass for  $1^{-}$  states with more exotic octet color configurations are all above 2 GeV. This is consistent with model predictions [30] for exotic hybrid meson ( $q\bar{q}g$ )  $1^{-}$  states also lying above 2 GeV due to repulsive color octet quark interactions. Finally, for any  $J^{PC}$  state, including the  $1^{-}$ , the computed masses (not shown) in both the triplet and the sextet diquark color representations are all heavier than in the singlet representation and comparable to the octet scheme results.

Two other effects which will modify our predicted tetraquark spectrum are spin splittings from the omitted hyperfine interaction and mixing of non-exotic tetraquarks with conventional  $q\bar{q}$  model states. From our previous hyperfine study [21] we generally expect small spin splittings, roughly 50 to 100 MeV. We also have just obtained preliminary results from a mixing analysis for scalar and pseudoscalar mesons with tetraquark systems and find the unmixed spectra are shifted from 50 to 100 MeV which yields an improved description of the observed light meson spectrum, particularly the  $\eta, \eta'$  states. Complete results will be published in a future communication.

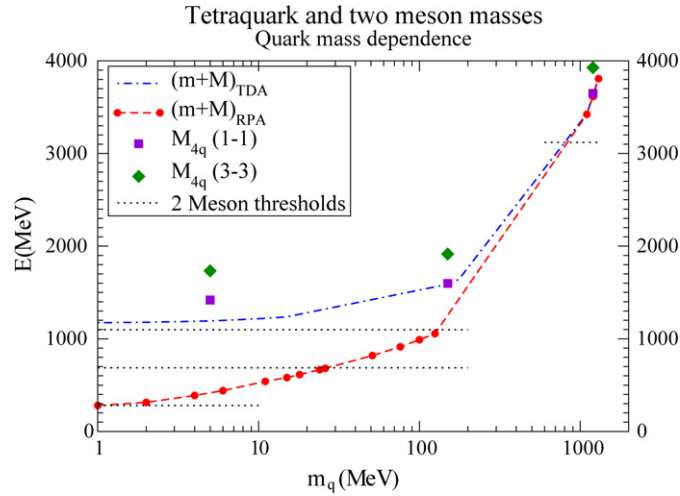


Fig. 4. Dotted lines, from bottom to top, are the  $\pi\pi$ ,  $\pi\eta$ ,  $\pi\eta'$ ,  $\pi\eta_c$  observed thresholds, respectively. The two other plots are the pseudoscalar  $m_\pi + M_{q\bar{q}}$  model predictions in the (chiral respecting) RPA and (chiral violating) TDA. The squares and diamonds correspond respectively to predicted scalar isoscalar tetraquark masses in the color singlet–singlet and triplet–triplet schemes. Note the two-meson calculation [20] has  $\sigma = 0.18 \text{ GeV}^2$ ,  $\alpha_s = 0$ , whereas our results use  $\sigma = 0.135 \text{ GeV}^2$ ,  $\alpha_s = 0.4$ , but the difference among both sets is known to be small for the ground state.

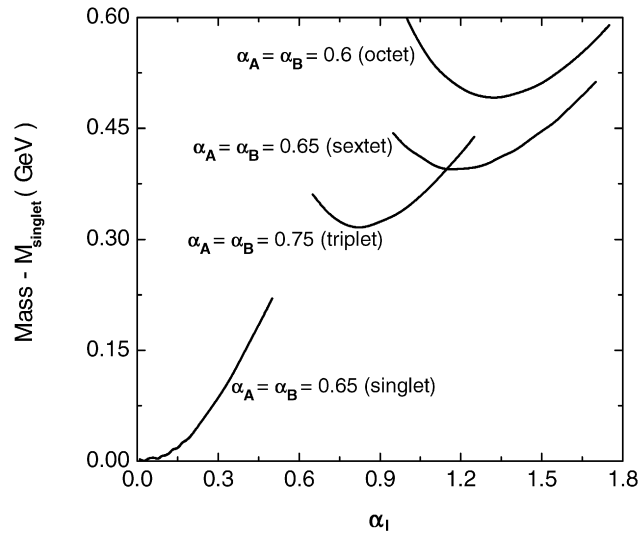


Fig. 5. Tetraquark mass of the ground state isoscalar  $0^{++}$  as a function of the intercluster variational parameter, for various color configurations. Note the more exotic color configurations are above 1.7 GeV.

It is interesting to document the current quark mass dependence of our results. This is illustrated in Fig. 4, where the calculated rest mass corresponding to different four quark systems (tetraquarks and two mesons) is displayed with one  $q\bar{q}$  pair fixed at a low 1–5 MeV while the other pair varies from 1 to 1300 MeV. Note the predicted  $c\bar{c}u\bar{u}$  tetraquark mass is relatively closer to the two meson decay threshold indicating a narrow decay width to the  $\pi\eta_c$  and  $\eta\eta_c$  channels (more so for  $b\bar{b}$ , not displayed). Also note a quark–meson exchange model [38] claims some  $J = 1$   $c\bar{c}u\bar{u}$  partners will be absolutely stable. Using  $m_c = 1.2 \text{ GeV}$  and  $m_q = 0, 110$  and  $150 \text{ MeV}$ , the lowest  $1^{+-}$  hidden-charm mass is 4.04, 4.10 and 4.15 GeV, respectively, for the molecular configuration and can be searched for in hidden charm decays (p-wave  $\eta_c\pi_0$ ,  $\eta_c\eta$  for example).

Fig. 5 displays the sensitivity of the scalar tetraquark mass to the variational parameters for each color scheme. The singlet–singlet configuration, at 1.28 GeV, is clearly the lightest, in agreement with previous predictions [39]. Similar results are obtained for other  $J^{PC}$  states which suggests that the lightest tetraquarks, including the  $\pi_1(1400)$  should it exist, are best interpreted as molecules of color singlets (the “extraordinary hadrons” [40]) and directly excitable via meson rescattering.

For further dynamical insight, Fig. 6 details contour plots of the probability densities using the hybrid (left) and tetraquark (right) variational wavefunctions. Note the depletion of the wavefunction at low-momentum, reflecting the rising confining potential at large distance, and the significantly different parton momentum distributions between hybrids and tetraquark systems. This difference in momentum distributions will produce distinct decay signatures which can be utilized to identify hybrids and tetraquarks as we now discuss.

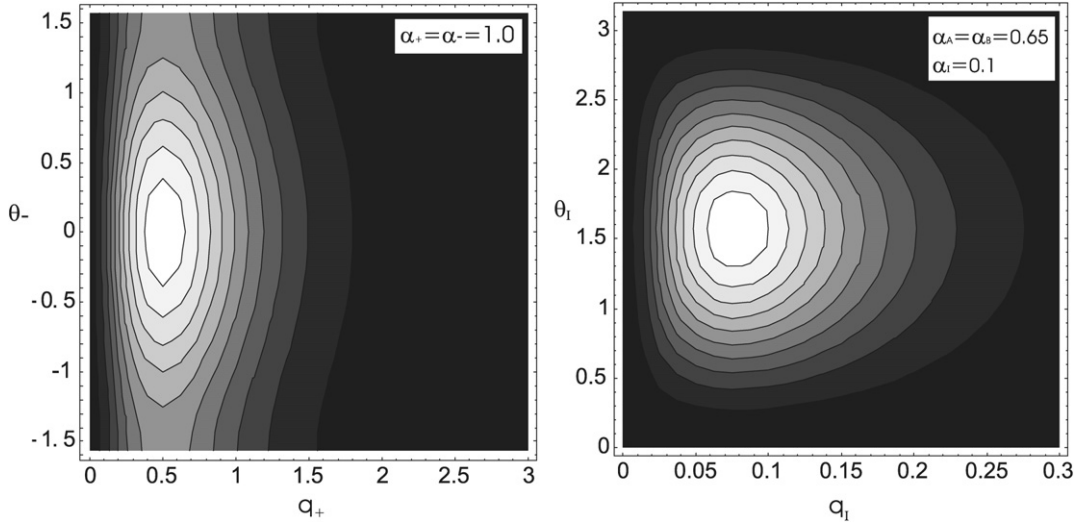


Fig. 6. Hybrid (left) and tetraquark (right) meson probability density contour plots. The left horizontal axis is half the momentum of the constituent gluon,  $q_+ = g/2$ . The left vertical axis is the angle between the  $q\bar{q}$  relative momentum  $q_-$  and the hybrid total angular momenta  $J$ . The right horizontal axis corresponds to the intracluster momentum  $q_I$  and the angle between this momentum and  $J$  for the tetraquark. Angles in radians, momenta in GeV.

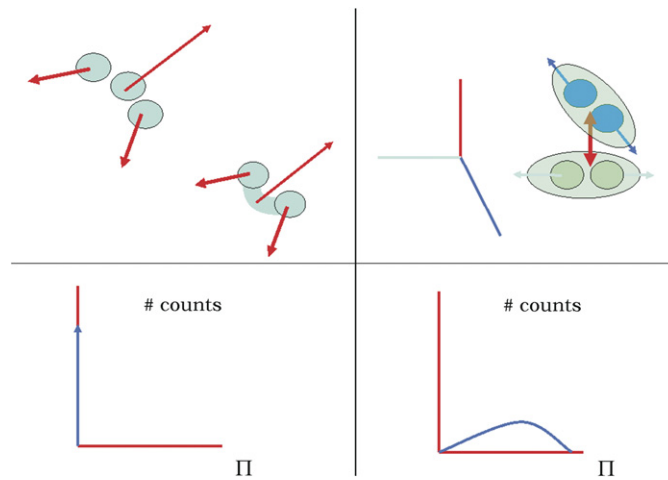


Fig. 7. Differences between internal in-plane three-body hybrid (top left) and off-plane tetraquark (top right) meson decays. From the Frank–Condon principle the internal momentum distribution is reflected in the momentum distribution of the final products yielding an off-plane final state momentum observable,  $\Pi$ , that is very different for  $q\bar{q}g$  (bottom left) and  $qq\bar{q}\bar{q}$  (bottom right) mesons.

It has been proposed [41] that  $1^{-+}$  exotic hybrid mesons decay preferentially to a meson pair in a relative s-wave, where one of the mesons is a p-wave (axial) meson. However that prediction was based on the Flux Tube model and not known to hold exactly in any limit. We have recently [30] detailed a less model dependent decay signature based upon the Franck–Condon principle of molecular physics, which predicts that the momentum distribution of decay products parallels the internal momentum distribution of the parent meson. This is an exact statement in the infinitely heavy quark limit, however it is also useful for physical quarks. Our previous application [30] was designed to distinguish  $q\bar{q}$  from  $q\bar{q}g$  mesons and is now generalized to the four-body problem. For two and three-body systems, in the  $cm$  partons' momenta are restricted to a plane, however for tetraquarks there are off-plane degrees of freedom which can be exploited as an identification signature (see the cartoon in Fig. 7). One observable sensitive to this is an exclusive measurement of decay to four mesons. By then determining their momenta  $\mathbf{p}_{i=1,2,3,4}$  in the  $cm$  of the exotic candidate, kinematic cuts can be applied for every two and three meson groups to eliminate intermediate two and three-body resonances that could confuse the analysis. From the pure (and much reduced) four-body decay sample count, one can construct the off-plane correlator,  $\Pi$ , for any three momenta which is the volume of the parallelepiped they form in momentum space,

$$\Pi(\mathbf{p}_1, \mathbf{p}_2, \mathbf{p}_3, \mathbf{p}_4) = \frac{((\mathbf{p}_1 \times \mathbf{p}_2) \cdot \mathbf{p}_3)^2}{\sqrt{|\mathbf{p}_1 \times \mathbf{p}_2| |\mathbf{p}_2 \times \mathbf{p}_3| |\mathbf{p}_1 \times \mathbf{p}_3| |\mathbf{p}_1 \times \mathbf{p}_4| |\mathbf{p}_2 \times \mathbf{p}_4| |\mathbf{p}_3 \times \mathbf{p}_4|}},$$

which has been normalized by the area of the six faces. This dimensionless off-plane correlator is useful for the very different scales involved in light and heavy quark physics, positive definite and invariant under permutation of the four momenta. In the  $cm$

system only three momenta are linearly independent. Taking them equal and along the edges of a cube yields  $\Pi = 8^{-1/4} = 0.59$ , with a more general maximum value close to 0.707. Therefore the value of the correlator event by event will be a random variable distributed between 0 and 0.707 and, with sufficient statistics, one could deduce the internal structure of the decaying resonance (bottom right plot of Fig. 7). This could then be compared to four-meson decays of established conventional and hybrid meson benchmarks, as distinguished using the procedure outlined in Ref. [30], which would be radically different (their  $\Pi$  volumes collapse to 0 in the heavy quark limit). While our correlator signature may not be feasible for certain reaction measurements, it should be useful for experiments having fixed initial quantum numbers, such as in  $e^+e^-$ , and high statistics.

Finally, we are currently calculating tetraquark decay widths to compare with both conventional and hybrid meson decays to two and multi-meson final states. These will also reflect hadronic structure differences and therefore aid exotic identification. Results will be reported in a future communication.

In conclusion, we submit that the observed  $1^{-+}$  exotics below 2 GeV are not color exotic hadrons but rather somewhat more conventional tetraquark molecular resonances involving color singlet  $q\bar{q}$  pairs. Our results also agree with lattice and other models predicting that color exotics (hybrid mesons, octet–octet, sextet–sextet and triplet–triplet tetraquarks) will have masses near and above 2 GeV. Finally, we have utilized the Frank Condon principle and the distinctive quark momentum distribution in a tetraquark to propose a new off-plane correlator measurement for identifying exotic hadrons.

## Acknowledgements

This work was supported in part by grants FPA 2004-02602, 2005-02327, PR27/05-13955-BSCH (Spain) and US DOE DE-FG02-97ER41048 and DE-FG02-03ER41260.

## References

- [1] G.S. Adams, et al., E852 Collaboration, Phys. Rev. Lett. 81 (1998) 5760.
- [2] S.U. Chung, et al., E852 Collaboration, Phys. Rev. D 60 (1999) 092001.
- [3] A.R. Dzierba, et al., Phys. Rev. D 73 (2006) 072001.
- [4] G. Adams, E862 Collaboration, hep-ex/0612062.
- [5] D.S. Carman, hep-ex/0612027v1.
- [6] J.N. Hedditch, et al., Phys. Rev. D 72 (2005) 114507.
- [7] M.S. Cook, H.R. Fiebig, Phys. Rev. D 74 (2006) 094501;  
M.S. Cook, H.R. Fiebig, Phys. Rev. D 74 (2006) 099901, Erratum.
- [8] T. Barnes, F.E. Close, E.S. Swanson, Phys. Rev. D 52 (1995) 5242.
- [9] F.E. Close, P.R. Page, Nucl. Phys. B 443 (1995) 233.
- [10] K. Waidelich, Diploma Thesis, North Carolina State University, 2001.
- [11] F. Iddir, L. Semlala, hep-ph/0511086.
- [12] F.J. Llanes-Estrada, S.R. Cotanch, Phys. Lett. B 504 (2001) 15.
- [13] F. Iddir, A. Le Yaouanc, L. Oliver, O. Pene, J.C. Raynal, S. Ono, Phys. Lett. B 205 (1988) 564.
- [14] S.U. Chung, E. Klempt, J.G. Korner, Eur. Phys. J. A 15 (2002) 539.
- [15] R. Zhang, Y.B. Ding, X.Q. Li, P.R. Page, Phys. Rev. D 65 (2002) 096005.
- [16] S.D. Bass, E. Marco, Phys. Rev. D 65 (2002) 057503.
- [17] A.P. Szczepaniak, M. Swat, A.R. Dzierba, S. Teige, Phys. Rev. Lett. 91 (2003) 092002.
- [18] A. Donnachie, P.R. Page, hep-ph/9807433.
- [19] F.J. Llanes-Estrada, S.R. Cotanch, Phys. Rev. Lett. 84 (2000) 1102.
- [20] F.J. Llanes-Estrada, S.R. Cotanch, Nucl. Phys. A 697 (2002) 303.
- [21] F.J. Llanes-Estrada, S.R. Cotanch, A.P. Szczepaniak, E.S. Swanson, Eur. Phys. J. C 33 (2004) S521;  
F.J. Llanes-Estrada, S.R. Cotanch, A.P. Szczepaniak, E.S. Swanson, Phys. Rev. C 70 (2004) 035202.
- [22] F.J. Llanes-Estrada, P. Bicudo, S.R. Cotanch, Phys. Rev. Lett. 96 (2006) 081601.
- [23] T.D. Lee, Particle Physics and Introduction to Field Theory, Harwood Academic Publishers, New York, 1990.
- [24] D. Zwanziger, Nucl. Phys. B 485 (1997) 185;  
D. Zwanziger, private communication.
- [25] G.S. Bali, K. Schilling, A. Wachter, Phys. Rev. D 56 (1997) 2566.
- [26] C.J. Morningstar, M.J. Peardon, Phys. Rev. D 60 (1999) 034509.
- [27] E. Eichten, K. Gottfried, T. Kinoshita, K.D. Lane, T.M. Yan, Phys. Rev. D 17 (1978) 3090;  
E. Eichten, K. Gottfried, T. Kinoshita, K.D. Lane, T.M. Yan, Phys. Rev. D 21 (1980) 313, Erratum.
- [28] A.P. Szczepaniak, P. Krupinski, Phys. Rev. D 73 (2006) 116002.
- [29] V. Dmitrasinovic, Phys. Rev. D 70 (2004) 096011.
- [30] I.J. General, F.J. Llanes-Estrada, S.R. Cotanch, Eur. Phys. J. C 51 (2007) 347.
- [31] S.R. Cotanch, I.J. General, P. Wang, Eur. Phys. J. A 31 (2007) 656.
- [32] R.L. Jaffe, Phys. Rev. D 15 (1977) 267.
- [33] A.T. Aerts, P.J. Mulders, J.J. de Swart, Phys. Rev. D 21 (1980) 1370.
- [34] A.M. Badalian, D.I. Kitoroage, Sov. J. Nucl. Phys. 47 (1988) 855, Yad. Fiz. 47 (1988) 1343.
- [35] L. Maiani, F. Piccinini, A.D. Polosam, V. Riquer, hep-ph/0512082v1.
- [36] F.J. Llanes-Estrada, Electronic proceedings of Alghero 2003, hep-ph/0311235.

- [37] E. Santopinto, G. Galata, *Phys. Rev. C* 75 (2007) 045206.
- [38] J. Vijande, F. Fernandez, A. Valcarce, B. Silvestre-Brac, *Eur. Phys. J. A* 19 (2004) 383.
- [39] J.D. Weinstein, N. Isgur, *Phys. Rev. D* 41 (1990) 2236.
- [40] R.L. Jaffe, hep-ph/0701038.
- [41] F.E. Close, P.R. Page, *Nucl. Phys. B* 443 (1995) 233.